A Real-World Test Problem for EMO Algorithms

A. Gaspar-Cunha, J.A. Covas

Dept. of Polymer Engineering, University of Minho, Guimarães, PORTUGAL
gaspar,jcovas@dep.uminho.pt

Abstract. In this paper, a real-world test problem is presented and made available for use by the EMO community. The problem deals with the optimization of polymer extrusion, in terms of setting the operating conditions and/or the screw geometry. The binary code of a computer program that predicts the thermomechanical experience of a polymer inside the machine, as a function of geometry, polymer properties and operating conditions, is developed. The program can be used through input and output data files, so that the parameters to optimize and the criteria evaluated data is communicated in both directions. Two distinct EMO algorithms are used to illustrate and test the optimization of this problem.

1. Introduction

Most, if not all, real-world optimization problems are multiobjective and their solution is not unique. Instead, a set of optimal solutions, denoted as Pareto optimal set, explicits the trade-off between the criteria considered. The aim of multiobjective optimization is not only to improve the fitness of the solutions as the search proceeds, but also to distribute them uniformly along the Pareto frontier. Since Evolutionary Algorithms, EAs, use a population of points, this can be used with great advantage to find the Pareto frontier. After the initial work of Schaffer [1], a considerable number of different Multi-Objective Evolutionary Algorithms, MOEA, have been proposed, good reviews being available in the literature [2,3].

A significant number of problems have been proposed to test the performance of those algorithms [2,3]. Generally, they use relatively simple mathematical functions, whose solutions are known *a priori* and require little computational effort. The aim is to test the robustness of any optimization algorithm solving problems that have Pareto fronts with a wide range of characteristics [4]. The topography of the search space of each problem under study can cause difficulty in the convergence to the Pareto optimal front and/or in preserving the diversity of the Pareto optimal solutions. The former can be due to the existence of properties such as multi-modality, deception, isolated optimum or collateral noise, whereas the latter is associated with convexity or non-convexity, discontinuity and non-uniform distribution of solutions. Specific test problems dealing with the existence of these characteristics have been suggested [2,4]. Test problems having demanding constraints causing additional difficulties to the MOEAs have also been developed [4,5]. Deb *et al.* [6] suggested a method to build scalable test problems with any number of decision variables and criteria. Three

different schemes were recommended, namely a multiple single-objective function approach, a bottom-up approach and a constraint surface approach. In the first case, different single-objective functions are used to create a multiobjective test problem, which corresponds to the usual practice by MOEAs researchers. The bottom-up approach uses a mathematical function describing the Pareto-optimal front in the objective space, which is used to define an overall search space and, therefore, to define the test problem. Finally, the constraint surface approach starts with the definition of the overall search space, for example a rectangular hyper-box. Then, constraints are added systematically to cut off regions from the box in order to create arbitrary Pareto-optimal hypersurfaces.

Since the ultimate goal of developing MOEAs is to solve real-world problems, it seems relevant to question whether the above test problems illustrate adequately the complex behavior of real-world applications. These, not only involve a considerable number of decision variables and criteria, as well as complicated relationships between them, but are also generally ill-posed (i.e., the inverse solution is often not unique) and combinatorial. Although EMO algorithms have been applied to practical problems [7,8], the current absence of accepted real-world test problems that can be used to test the algorithms in a real environment is evident.

Therefore, the aim of the present work is to propose a real-world test problem with attractive features in terms of EMOAs, more specifically, the optimization of the polymer extrusion process, as a test problem to be adopted by the scientific community. A modeling routine of the process in binary code and two data files are available through the Internet (*www.dep.uminho.pt/pp/index.php3?gaspar@dep.uminho.pt*). The first is used to transfer from the EMO algorithm to the modeling routine the values of the solutions proposed. The second file passes on from the modeling routine to the EMO algorithm the values of the criteria selected. The test problem proposed will be optimized using two different EMO algorithms.

2. Polymer Extrusion as a Test Problem

2.1. The Process

Extrusion is one of the most industrially relevant processing techniques used by companies producing plastics parts. It is used to manufacture mass-consumption products such as tubing, pipes and profiles for the building, automotive and medical industries, film and sheet for packaging and agricultural applications, filaments and fibers for textiles, electrical wires and cables. Plastics compounding, i.e., the preparation of raw materials with advanced properties, through the incorporation of additives to a polymer matrix, polymer modification, or polymer blending, are also carried out in extruders.

In a typical single screw extruder (see Figure 1) an Archimedes-type screw rotates at a given frequency inside a heated barrel. The aim of the process is to receive the solid pellets at the inlet (hopper), melt and mix the material, and pump it at a constant

rate through the die, which is coupled to the other end of the barrel, in order to produce an extrudate with a prescribed cross-section. The material will be subsequently cooled downstream, printed/decorated, coiled or cut in regular lengths, using other machines that are not represented in Fig. 1.

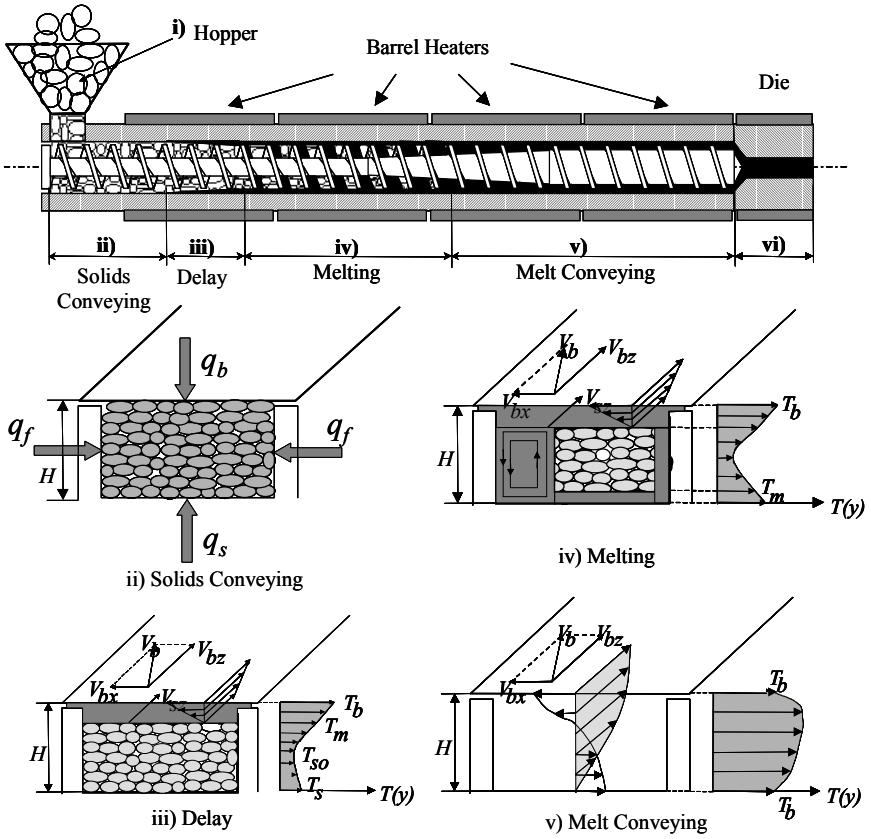

Fig. 1. Plasticating sequence inside a polymer extruder

From a thermomechanical point of view, as the material progresses along the screw it is subjected to various mechanisms, which are also illustrated in Figure 1. The polymer pellets in the hopper (i) flow into the barrel by action of gravity. Friction between the polymer and the adjacent metallic walls will drag the material downstream, along the helical screw channel (ii). Heat conduction and dissipation will melt the material closer to the inner barrel wall (this is often known as *delay* in melting) (iii). When the rate of melting becomes sufficiently significant, a specific melting mechanism develops, the melt and solid components segregating from each other (iv). The resulting melt is mixed and conveyed (v) towards the die (adopting a helical velocity profile along the screw channel), where it is shaped into the desired cross-section (vi). Detailed phenomenological and mathematical descriptions of this sequence of events can be found elsewhere [9-11]. In addition to the complexity of the process, polymer melts are viscoelastic, i.e., they exhibit a combination of solid-

like and liquid-like behavior (which is time, temperature, deformation rate and stress dependent). For the sake of simplicity, a power law viscous constitutive equation is often adopted (where the power index, n quantifies the non- melt character).

For a given equipment geometry and polymer system the main operating variables are the screw rotation frequency and the barrel set axial temperature profile. Upon starting the manufacture of a new product, it is often necessary to define the best screw and the operating conditions that will process most efficiently the polymer selected. Process performance is usually evaluated in terms of mass output, mixing quality, length of screw required for melting, power consumption, average residence time inside the extruder and level of viscous dissipation.

2.2. The Modeling Routine

The solution of the direct problem involves predicting the value of the performance variables identified above for a given input set of material/geometry/operating conditions. Since each of the individual process stages has to be described mathematically, use of proven models was made, whenever possible [9-12].

Gravity flow in the hopper (Fig.1-i) was modeled considering the existence of a sequence of vertical and/or convergent columns subjected to static loading conditions [13]. The vertical pressure profile can be determined from a force balance on an elemental slice of the bulk [14]. We assumed the transport of a non-isothermal elastic solid plug with heat dissipation at all surfaces in the initial screw turns (Fig.1-ii). The computation of the solids temperature takes into account the contribution of conduction from the hot barrel, of friction near the polymer/metal interfaces, and of heat convection along the channel due to polymer motion [15,16]:

$$V_{sz}\,\frac{\partial T(y)}{\partial z} = \alpha_s\,\frac{\partial^2 T(y)}{\partial y^2} \tag{1}$$

where V_{sz} is the solid bed velocity, $T(y)$ is the cross temperature profile (direction y) and α_s is the thermal diffusivity of the solid plug. The pressure generated can be determined from force and torque balances made on differential down-channel elements [15].

$$P_2 = P_1 \exp\left[\int_{z_1}^{z_2}\left(\frac{B_1 - A_1 K}{B_2 + A_2 K}\right)dz\right] \tag{2}$$

where P_1 and P_2 are the pressures at down-channel distances z_1 and z_2, respectively, and A_1, A_2, B_1, B_2 and K are constants that are dependent on the friction coefficients and geometry.

The higher temperatures near to the inner barrel wall will cause the formation of a melt film (Fig. 1-iii) [12,17,18]. The film thickness and temperature can be computed from the momentum and energy equations, assuming heat convection in the down-channel and radial directions and heat conduction in the radial direction [19].

$$\frac{\partial P}{\partial x} = \frac{\partial}{\partial y}\left(\eta \frac{\partial V_x}{\partial y}\right) \tag{3}$$

$$\frac{\partial P}{\partial y} = 0 \tag{4}$$

$$\frac{\partial P}{\partial z} = \frac{\partial}{\partial y}\left(\eta \frac{\partial V_z}{\partial y}\right) \tag{5}$$

$$\rho_m \; c_p \; V_z(y) \frac{\partial T}{\partial z} = k_m \; \frac{\partial^2 T}{\partial y^2} + \eta \; \dot{\gamma}^2 \tag{6}$$

where ρ_m, c_p and k_m denote melt density, specific heat, and thermal conductivity, respectively, and η is the melt viscosity, which follows a temperature dependent power law:

$$\eta = k \; \exp\left[-a\left(T - T_0\right)\right] \dot{\gamma}^{n-1} \tag{7}$$

where k and n are the consistency and power law indices, respectively, a is the temperature shift factor, T_0 is the reference temperature, and $\dot{\gamma}$ is given by:

$$\dot{\gamma} = \left[\left(\frac{\partial V_x}{\partial y}\right)^2 + \left(\frac{\partial V_z}{\partial y}\right)^2\right]^{1/2} \tag{8}$$

$$\int_0^{\delta_C} V_x(y) \, dy = 0 \tag{9}$$

The melting step was described mathematically adopting the 5-regions model proposed Lindt *et al* [20,21], shown in Fig. 1-iv (development of a melt pool near the left screw flight, of melt films near the barrel and screw walls and a solid bed that is vanishing slowly). Treatment of each region requires different forms of the momentum and energy equations, coupled to the relevant boundary conditions**.** The flow of the melt films can be described by equations (3) to (8), together with specific boundary conditions and a condition for cross-channel flow (equation 9). Flow in the melt pool is taken as two-dimensional, hence equations (5), (6) and (8) are replaced, respectively, by:

$$\frac{\partial P}{\partial z} = \frac{\partial}{\partial y}\left(\eta \frac{\partial V_z}{\partial x}\right) + \frac{\partial}{\partial y}\left(\eta \frac{\partial V_z}{\partial y}\right) \tag{10}$$

$$\rho_m \, c_p \, V_z(y) \frac{\partial T}{\partial z} = k_m \left(\frac{\partial^2 T}{\partial x^2} + \frac{\partial^2 T}{\partial y^2} \right) + \eta \, \dot{\gamma}^2 \tag{11}$$

$$\dot{\gamma} = \left[\left(\frac{\partial V_x}{\partial y} \right)^2 \left(\frac{\partial V_z}{\partial y} \right)^2 + \left(\frac{\partial V_x}{\partial y} \right)^2 \right]^{1/2} \tag{12}$$

Melt conveying (Fig.1-v) is identical to flow in the melt pool of the melting stage upstream, i.e. a non-isothermal two-dimensional flow of a power-law fluid develops. Hence, equations (3), (4), (10) and (11) remain valid, if coupled to updated boundary conditions [19]. Distributive mixing was taken into consideration. Its intensity is related to the growth of the interfacial area between any two adjacent fluid elements, which depends on the local melt shear strain and average residence time. We adopted a weighted-average total strain function, WATS [19,22,23], as a simple criterion to estimate the degree of mixing.

Finally, pressure flow in the die (Fig.1-vi) was computed assuming that the latter is made of successive channels with uniform cross-section in the downstream direction, the non-isothermal two-dimensional flow of a power law fluid taking place (equations (1), (9) and (10) are solved by finite differences).

The global plasticating extrusion model links sequentially the above stages, using appropriate boundary conditions, and ensuring coherence of the physical phenomena between any two adjacent zones. The calculations are performed for small down-channel increments along the screw and die, using a tentative output. Convergence is attained when the pressure drop predicted at the die exit becomes sufficiently small. Two algorithms are used in sequence. First, it is necessary to establish an interval (two values for output) that contains the solution, using a bracketing algorithm [24]. Then, Brent's algorithm is used to find the solution for the output inside this interval [25]. Using a Personal Computer with an Intel Celeron at 800 MHz, is takes typically one minute to compute one solution.

2.3. Typical Process Response

The Output – Pressure relationship for a typical extruder and die is shown in Figure 2 (Leistritz LSM 34 extruder and die described in Fig. 5, processing a High Density Polyethylene). The effect of increasing the screw speed and the die set temperature on the response of each of these components is also represented. The effective operating point corresponds to the intersection between the curves valid for each component, i.e., when the extruder (operating at specific conditions) is coupled to the die (kept at a certain temperature), one output is obtained as a result of a pressure generated by the extruder, which obviously equals the pressure drop in the die.

Table 1 presents the typical extruder response when the screw speed is gradually increased from 20 to 50 rpm, for constant system and polymer properties. The values of all the criteria considered increase with increasing screw speed, but in many cases in a nonlinear fashion. Temperature related criteria depend on material temperature development inside the extruder, which in turn results from the contribution of heat transfer and viscous dissipation. The former depends on the set temperatures and residence time (proportional to output), while the latter depends on average velocity (again, output) and material viscosity. Velocity related criteria (output, power consumption, WATS) depend on pressure generation and on the shape of the velocity fields.

Table 1. Influence of screw speed on the extruder performance.

Criteria	**Screw Speed (rpm)**						
	20	30	*50.0%*	40	*33.3%*	50	*25.0%*
Output (kg/hr)	3.15	4.92	*56.0%*	6.67	*35.8%*	8.46	*26.8%*
Length for Melting (m)	0.46	0.61	*32.9%*	0.66	*8.5%*	0.69	*5.1%*
Melt Temperature (ºC)	174.1	177.1	*1.7%*	180.2	*1.8%*	183.3	*1.7%*
Power Consumption (W)	794.5	1140.8	*43.6%*	1558.4	*36.6%*	2075.7	*33.2%*
WATS	195.2	219.4	*12.4%*	254.8	*16.1%*	240.4	*-5.6%*
T_{avg}/T_b	1.03	1.05	*1.6%*	1.06	*1.5%*	1.08	*1.6%*
T_{max}/T_b	1.08	1.12	*4.1%*	1.16	*3.5%*	1.20	*3.3%*

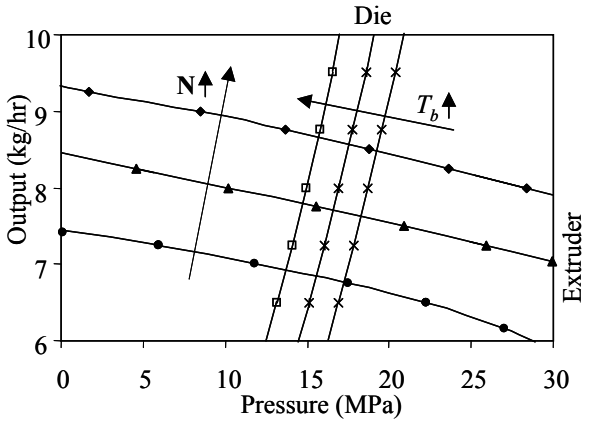

Fig. 2. Operating point of an extruder-die combination

Table 2 is similar to Table 1, but now the operating conditions have been kept fixed, the channel depth of the last section of the screw being increased. An increase in the cross-section of the screw channel favors output, but the corresponding decrease in residence time compromises the melting and mixing efficiencies.

Finally, Fig. 3 illustrates the evolution of pressure, melting (in terms of reduced solid bed width, X/W), average melt temperature and mechanical power consumption along the machine. The results produced by this modeling routine were assessed experimentally, using different polymers and operating conditions [19]. Generally, the predicted values are within ± 10% of the experimental data.

Table 2. Influence of channel depth on the extruder performance.

Criteria	Internal Screw Diameter/Channel Height (mm)						
	32	30	*-6.3%*	28	*-6.7%*	26	*-7.1%*
	2	3	*50.0%*	4	*33.3%*	5	*25.0%*
Output (kg/hr)	8.46	11.82	*39.7%*	15.45	*30.7%*	18.48	*19.6%*
Length for Melting (m)	0.69	0.83	*19.4%*	0.89	*7.0%*	0.89	*0.0%*
Melt Temperature (ºC)	183.3	182.9	*-0.2%*	176.7	*-3.4%*	178.7	*1.1%*
Power Consumption (W)	2075.7	1920.8	*-7.5%*	1763.6	*-8.2%*	1906.8	*8.1%*
WATS	240.4	54.4	*-77.4%*	12.4	*-77.2%*	11.0	*-11.3%*
T_{avg}/T_b	1.08	1.08	*-0.2%*	1.04	*-3.4%*	1.05	*1.1%*
T_{max}/T_b	1.20	1.19	*-1.3%*	1.18	*-0.2%*	1.18	*-0.3%*

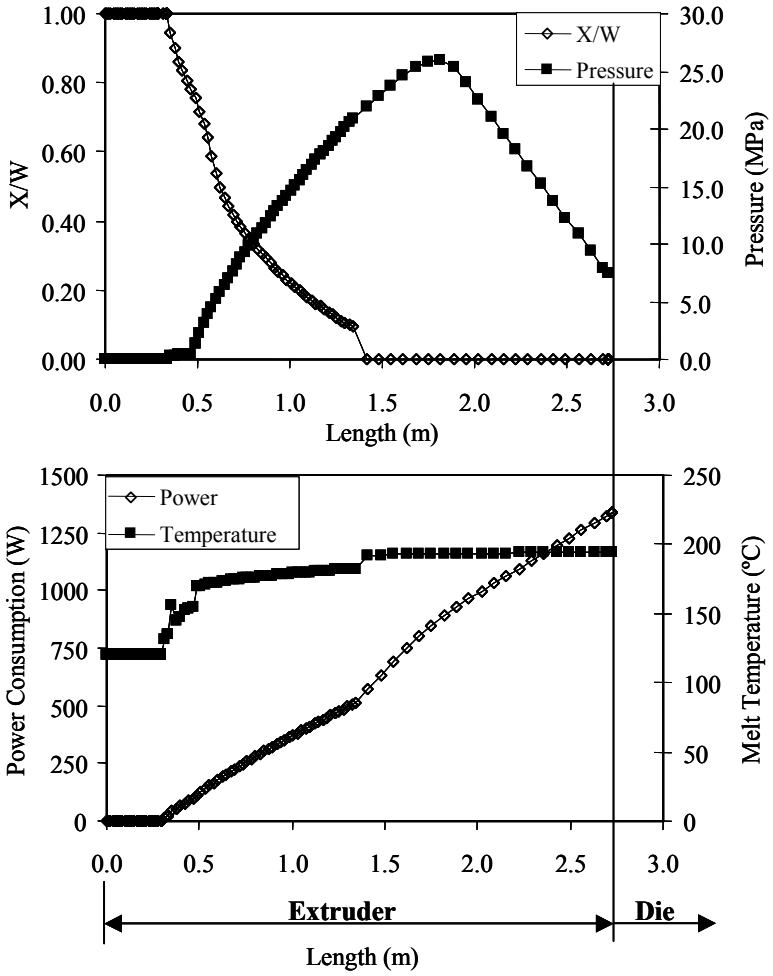

Fig. 3. Evolution of some extrusion parameters along the screw and die.

2.4. Using the Test Problem

The polymer extrusion test problem is accessible at *www.dep.uminho.pt/pp/index.php3?gaspar@dep.uminho.pt,* where detailed instructions are also given. Figure 4 illustrates how it can be inserted in a MOEA sequence. After defining which variables are to be optimized and which process criteria are to be used, any MOEA needs to evaluate a proposed solution. In order to accomplish this, it transfers to the extrusion program, via the text file "extr.var", the input values of the variables corresponding to that solution and receives, via the text file "extr.cri", the corresponding values of the process criteria. The following criteria are available for consideration: mass output (Q), degree of mixing ($WATS$), length of screw required to melt the polymer (Z_T), mechanical power consumption ($Power$), melt temperature at die exit (T_{exit}) and viscous dissipation (which can be estimated from the average melt temperature/barrel temperature and/or maximum temperature/barrel temperature). Usually, the first two are to be maximized, while the remaining should be kept as low as possible.

The extrusion program "extr.exe" requires as input data operating conditions, namely screw speed (N) and barrel temperatures in three zones (T_{b1}, T_{b2}, T_{b3}), and geometrical parameters, such as the internal diameter of sections 1 and 3 (D_1, D_3), the length of sections 1 and 2 (L_1, L_2), the screw pitch (P) and the flight thickness (e) (see Figure 5). These are stored in the data file "extreq". The file "extrmat" contains the material properties, which include solid and melt densities, solid and melt thermal conductivities, heat capacity, friction coefficients and melt viscosity.

In short, six files can be downloaded from the Internet: the modeling program "extr.exe", the polymer properties "extrmat" and the extruder geometry and operating conditions "extreq" databases, the parameters to optimize "extr.var" and the criteria "extr.cri" files, and the text file "readme" with instructions on the working of the test problem.

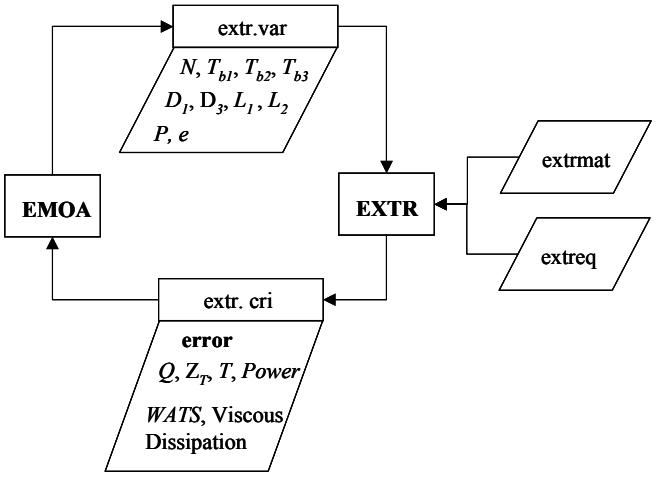

Fig. 4. Scheme used to link an MOEA with the extrusion test problem

3. Optimization

3.1. Reduced Pareto Set Genetic Algorithm with Elitism (RPSGAe)

The test problem will be used by two optimisation algorithms, the NSGA-II, an elitist non-dominated sorting GA, developed by Deb *et al* [27], and the RPSGAe, proposed by the authors [28]. The first method uses simultaneously an elite preservation strategy and an explicit diversity preserving mechanism. First, an offspring population is created using the parent population, both of size N. These populations are combined together to form a single population of size $2N$. Then, a classification of the population using a non-dominated sorting is performed. Finally, the new population is filled with the individuals of the best fronts, until the size of the population becomes equal to N. If the population becomes bigger than N, a niching strategy is used to select the individuals of the last front. The RPSGAe algorithm incorporates a solution clustering technique, in order to reduce the number of solutions on the efficient frontier while maintaining their characteristics intact. In each generation, the N population individuals are reduced to a pre-defined number of ranks (r=1,2,...,N_{Ranks}), and the value of the objective function is calculated using a ranking function. Simultaneously, an external elitist population is maintained, with the aim of preserving the best solutions already found and of incorporating periodically some of them in the main population. The number of ranks influences the performance of the algorithm and must be set carefully [28].

3.2. Case Studies

Two case studies will be studied (see also Fig. 5). The first deals with the optimization of the operating conditions (for fixed polymer properties and extruder geometry). The aim is to define the screw speed (N) and the barrel temperature (in zones T_{b1}, T_{b2} and T_{b3}) that maximize the mass output (Q) and the mixing quality ($WATS$), and minimize the length of screw required to melt the polymer (Z_T), the mechanical power consumption ($Power$) and the melt temperature at die exit (T_{exit}). Fig. 5.A) indicates the range of variation of the parameters to optimize between square brackets. Three runs will be performed. The first uses the five criteria, while the remaining will be performed taking into account two criteria at a time, namely output and power consumption, and output and WATS, respectively. The NSGA-II algorithm will use a population size of 100, 50 generations, a roulette wheel and tournament selection strategies, a crossover probability of 0.8 and a mutation probability of 0.05 a random seed of 0.5. The RPSGAe algorithm introduces the number of ranks (N_{ranks}, 30) and the limits of indifference of the clustering technique, 0.01. These values have been defined in previous studies of the algorithm [28]. In both cases, a real codification of the variables is used, together with SBX crossover and polynomial mutation operators.

The second case study deals with the optimization of the screw geometrical parameters, *i.e.*, with screw design, which is an emerging research area in polymer

processing [30]. The parameters to optimize are the screw length of zones 1 and 2 (L_1 and L_2), the internal screw diameter of sections 1 and 3 (D_1 and D_3), the screw pitch (P) and the flight thickness (e), whose range of variation is indicated between square brackets in Fig. 5.B). The operating conditions are fixed at N=50rpm and T_i=170ºC. Output maximization and power consumption minimization will be used as criteria. The same algorithms parameters were adopted here.

In both case studies it was also necessary to consider some constraints for the criteria. For example, the mechanical power that is available by the extruder for screw rotation is limited (9200 W). The thermal stability of polymers is also limited, henceforth a maximum temperature of 270ºC was allowed. The length of screw required for melting must also be constrained (0.9 m), since a sufficiently long melt conveying zone, for pressure generation and distributive mixing, must be guaranteed. A small value for the fitness is attributed to any solution violating these constraints.

3.3. Results and Discussion

The results obtained for the optimization of the operating conditions of the single screw extruder of Fig. 5.A) considering five criteria are presented in Fig. 6, for the two algorithms. All criteria are plotted against output, which was taken as the most important. As expected, output, length of screw required for melting and power consumption are conflicting. All Pareto frontiers are well defined, with the exception of that concerning melt temperature, since its interaction with other variables is very strong. There are some points that appear to be dominated in one Pareto frontier, but they are, certainly, non-dominated in another. Fig. 7.A) refers to the maximization of output and the minimization of power consumption. Both algorithms define clearly an optimal Pareto frontier evidencing the contradicting nature of these criteria. When mixing degree (WATS) and output are selected as the two criteria – Fig. 7.B) – the optimal Pareto frontier becomes discontinuous.

The total number of function evaluations was fixed at 4000 for both algorithms. The performance of the two algorithms was compared using the S-metric proposed by Zitzler [31]. Table 3 presents the results obtained after running each algorithm 5 times using different initial populations. The performance of NSGAII appears to be slightly better than that of RPSGAe, but the latter is more stable, as shown by the considerably lower standard deviation.

Table 3. Comparison results (S-metric).

	NSGAII with Roulette-wheel	**NSGAII with Tournament selection**	**RPSGAe**
S-metric average	0.076945	0.076497	0.07536
Standard deviation	0.026167	0.0268	0.000806

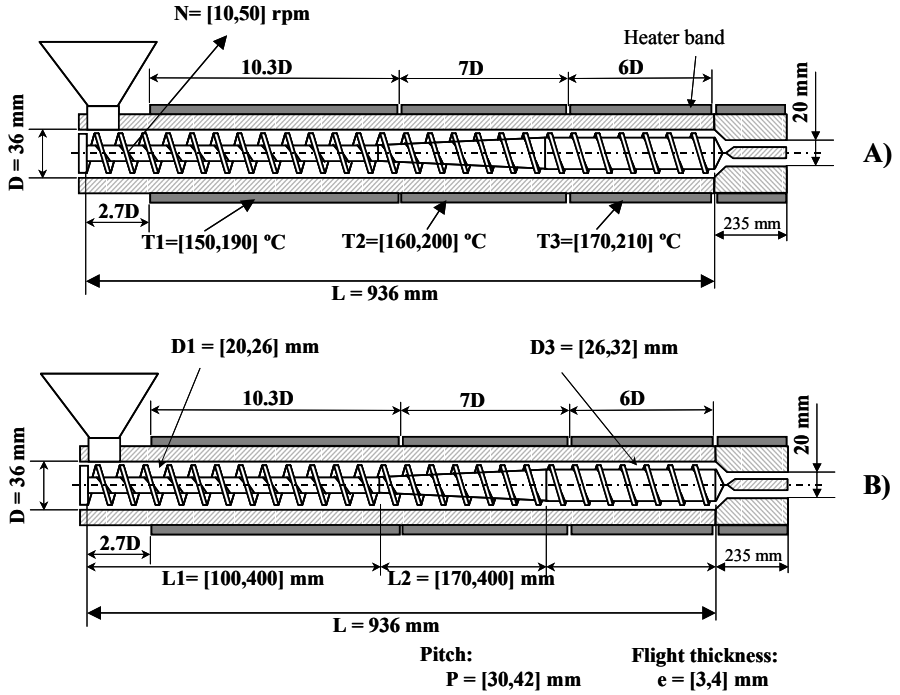

Fig. 5. Case studies A) Optimization of the operating conditions B) Screw design (*L* is the total screw length and *D* is the internal barrel diameter).

The results concerning screw design are presented in Fig. 8. The Pareto frontiers are quite distinct from the previous ones, because the geometry influences significantly the output, the power consumption and the mixing degree. However, both optimization algorithms produce coherent and similar results.

4. Conclusions

We have suggested and made available through the Internet a real-world test problem for multiobjective optimization, polymer extrusion. The problem can focus the optimization of the operating conditions, and/or the design of a screw for a particular application. As a test problem for EMO algorithms, it contains a variety of interesting characteristics, such as the possibility of using a variable number of criteria and parameters, of considering criteria with and without constraints, and of producing continuous, discontinuous and concave Pareto frontiers. Therefore, polymer extrusion could be a valid benchmark problem for multiobjective optimization algorithms, together with the available test functions.

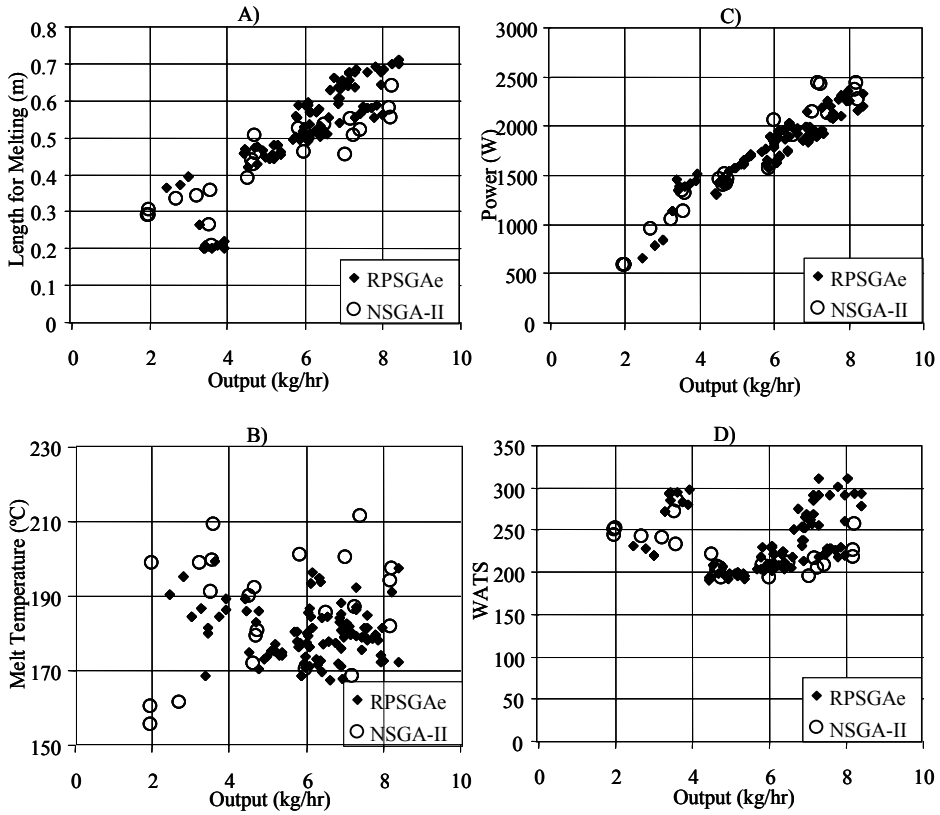

Fig. 6. Optimization of the operating conditions using five criteria

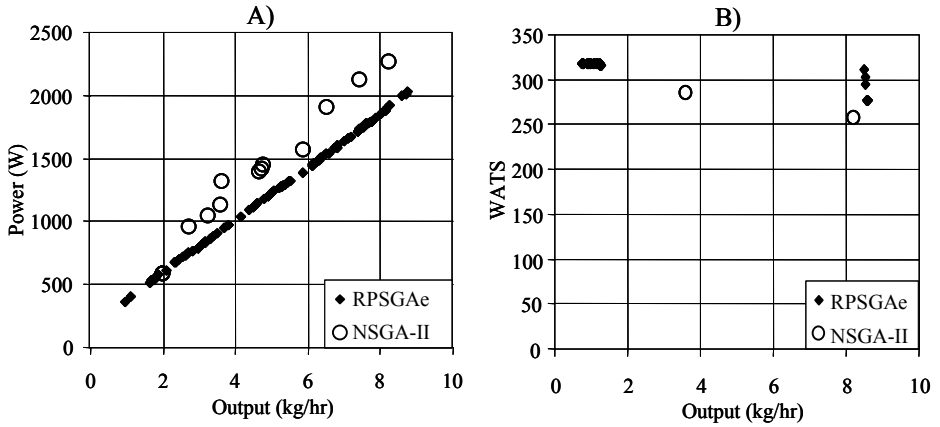

Fig. 7. Optimization of the operating conditions. A) Maximizing the output and minimizing the power consumption; B) Maximizing the output and the WATS.

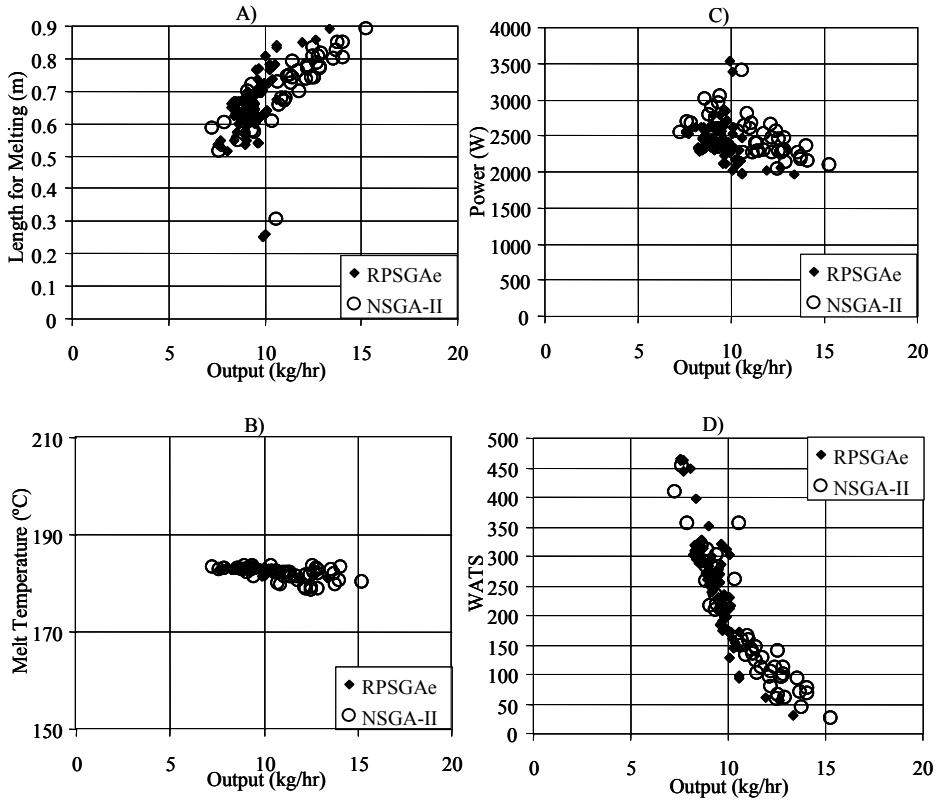

Fig. 8. Screw design using five criteria.

References

1. Schafer, J.D.: Some Experiments in Machine Learning Using Vector Evaluated Genetic Algorithms, Ph. D. Thesis, Nashville, TN, Vanderbilt University (1984)
2. Deb, K.: Multi-Objective Optimisation using Evolutionary Algorithms, Wiley (2001)
3. Coello Coello, C.A., Van Veldhuizen, D.A., Lamont, G.B.: Evolutionary Algorithms for Solving Multi-Objective Problems, Kluwer (2002)
4. Deb, K.: Multi-objective Genetic Algorithms: Problems Difficulties and Construction of Test Problems, Evolutionary Computation Journal, 7 (1999) 205-230
5. Deb, K., Pratap, Meyarivan, T: Constrained Test Problems for Multiobjective Evolutionary Optimization, Proceedings of the First Int. Conf. On Evolutionary Multiobjective Optimization (EMO-2001), Zurich, Switzerland (2001) 284-298
6. Deb, K., Thiele, L., Laumanns, M., Zitzler, E.: Scalable Multi-Objective Optimization Test Problems, Proceedings of the 2002 IEEE Congress on Evolutionary Computation (CEC 2002) (2002)
7. Eckart Zitzler, Kalyanmoy Deb, Lothar Thiele, Carlos A. Coello Coello, David Corne (Eds.): Evolutionary Multi-Criterion Optimization, First International Conference, EMO 2001, Zurich, Switzerland, March 2001, Proceedings, Lecture Notes in Computer Science (LNCS) Vol. 1993, Springer-Verlag, Berlin (2001)

8. Deb, K., Thiele, L., Yen, G., Zitzler, E. (eds.): Special Track on Evolutionary Multi-Objective Optimization (EMO), Congress on Evolutionary Computation (CEC), Honolulu, Hawaii (2002)
9. Amellal, K., Lafleur, P.G., Arpin, B.: Computer Aided Design of Single-Screw Extruders, in A.A. Collyer, L.A. Utracki (eds): Polymer Rheology and Processing, Elsevier (1989) 277-317
10. Rauwendaal, C.: Polymer Extrusion, Hanser Publishers, Munich (1986)
11. O´Brian, K.: Computer Modelling for Extrusion and Other Continuous Polymer Processes, Carl Hanser Verlag, Munich (1992)
12. Agassant, J.F., Avenas, P., Sergent, J.: La Mise en Forme des Matiéres Plastiques, 3rd edn, Lavoisier, Paris (1996)
13. Stevens, M.J., Covas, J.A.: Extruder Principles and Operation, 2nd ed., Chapman & Hall, London (1995)
14. Walker, D.M.: An Approximate Theory for Pressures and Arching in Hoppers, Chem. Eng. Sci., 21 (1966) 975-997
15. E. Broyer , Z. Tadmor, Solids Conveying in Screw Extruders – Part I: A modified Isothermal Model, Polym. Eng. Sci., 12, pp. 12-24 (1972).
16. Tadmor, Z., Broyer, E.: Solids Conveying in Screw Extruders – Part II: Non Isothermal Model, Polym. Eng. Sci., 12 (1972) 378-386
17. Tadmor, Z., Klein, I.: Engineering Principles of Plasticating Extrusion, Van Nostrand Reinhold, New York (1970)
18. Kacir, L., Tadmor, Z.: Solids Conveying in Screw Extruders – Part III: The Delay Zone, Polym. Eng. Sci., 12 (1972) 387-395
19. Gaspar-Cunha, A.: Modelling and Optimisation of Single Screw Extrusion, Ph. D. Thesis, University of Minho, Guimarães, Portugal (2000)
20. Lindt, J.T., Elbirli, B.: Effect of the Cross-Channel Flow on the Melting Performance of a Single-Screw Extruder, Polym. Eng. Sci, 25 (1985) 412-418
21. Elbirli, B., Lindt, J.T., Gottgetreu, S.R., Baba, S.M.: Mathematical Modelling of Melting of Polymers in a Single-Screw Extruder, Polym. Eng. Sci., 24 (1984) 988- 999
22. Pinto, G., Tadmor, Z.: Mixing and Residence Time Distribution in Melt Screw Extruders, Polym. Eng. Sci., 10 (1970) 279-288
23. Bigg, D.M.: Mixing in a Single Screw Extruder, Ph. D. Thesis, University of Massachusetts (1973)
24. Press, W.H., Teukolsky, A.A., Vetterling, W.T., Flannery, B.P.: Numerical Recipes in C: The Art of Scientific Computation, 2nd edition, Chapter 9, Cambridge University Press, Cambridge (1992)
25. Brent, R.P.: Algorithms for Minimization without Derivatives, Englewood Cliffs, Prentice-Hall, New Jersey (1973)
26. Web Page: www.dep.uminho.pt/pp/index.php3?gaspar@dep.uminho.pt (2002)
27. Deb, K., Pratap, A., Agrawal, S., Meyarivan, T.: A Fast and Elitist Multi-Objective Genetic Algorithm: NSGAII, IEEE Transactions on Evolutionary Computation, 6 (2002) 182-197
28. Gaspar-Cunha, A.: Reduced Pareto Set Genetic Algorithm (RPSGAe): A Comparative Study, The Second Workshop on Multiobjective Problem Solving from Nature (MPSN-II), Granada, Spain (2002)
29. Kanpur Genetic Algorithm Laboratory (KANGAL) web page: http://www.iitk.ac.in/kangal/soft.htm
30. Gaspar-Cunha, A.; Covas,J.A.: The Design of Extrusion Screws: An Optimisation Approach, Intern. Polym. Process., 16, pp. 229-240 (2001)
31 Zitzler, E.: Evolutionary Algorithms for Multiobjective Optimization: Methods and Applications, PhD Thesis, Swiss Federal Institute of Technology (ETH), Zurich, Switzerland (1999)